

1

1 2 3 4 5 6 7
8 9 10

•

•

$$\vdots$$

9

9

가 4, CT 4, (MRI) 6 CT, MR

: 가 6 , 가 3 , 50 88 62 .

가 4 가 2 , 1 , 1
1 .

1, 2, 3, 6 . MRI 6 T1

: 가 .

가 .

(1, 2). Bloom (3) 70 가

가

가 (4, 5)

9

가

8
9가
10

2005 4 7

2005 5 23

1996 1 2004 8

9

9 , 4 , CT

4 , (MRI) 6 . CT MRI

Table 1

MRI T1 (TR/TE, 400 - 50 88 가 6 , 가 3

560/12 - 25) T2 (TR/TE, 1600 - 5083/60 - 119) 62 .

Gadolinium - DTPA T1

가 4 가

2 , 1 , 1

1

CT , MR

MR T1 T2

2 , 2 , 1 , 1 , 1 ,

1 1 3 , 6

CT

Table 1. Clinical and Imaging Findings in Nine Patients with Metastatic Bone Tumors with Sunburst Periosteal Reaction

Age (y)/ Sex	Origin of Primary Tumor	Symptom	Operative history	Kind of Imaging	Imaging Findings		
					Metastatic site	Type of metastasis	Signal intensity
53/F	Stomach	Painful swelling of index	Gastrectomy (1 yr)	Radiography MR Bone scan	Phalanx	Osteolytic	Intermediate on T1-WI, Heterogenous high on T2-WI, Good homogenous enhancement
69/M	Stomach	Lower leg pain	Gastrectomy (4 yr)	Radiography MR Bone scan	Tibia	Osteoblastic	Intermediate on T1-WI, Heterogenous high on T2-WI Good homogenous enhancement
50/M	Stomach	Chest pain	-	Radiography CT MR	Rib	Osteoblastic	Intermediate on T1-WI Heterogenous high on T2-WI Good homogenous enhancement
57/M	Stomach	Upper arm pain	-	Radiography	Humerus	Osteolytic	
70/F	Lung	Shoulder pain	-	Radiography CT MR	Scapula	Osteoblastic	Intermediate on T1-WI, Heterogenous high on T2-WI Mild homogenous enhancement
50/F	Lung	Pelvic pain	-	Radiography CT MR	Ilium	Osteolytic	Intermediate on T1-WI, Heterogenous high on T2-WI Good homogenous enhancement
88/M	Prostate	Back pain	-	Radiography CT Bone scan	Lumbar spine	Osteoblastic	
58/M	HCC	Upper arm pain and swelling	-	Radiography MR Bone scan	Humerus	Osteoblastic	Intermediate on T1-WI, Heterogenous high on T2-WI Good homogenous enhancement
67/M	Unknown	Shoulder pain		Radiography	Scapula	Osteoblastic	

Note. - Dash(-) indicates absent

4
가
MRI 6 T1 가
3 1
, T2 30%
(6).
(7).



Fig. 1. A 69-year-old man with stomach adenocarcinoma.

A. Plain radiograph shows a large, destructive bone-forming lesion in the epiphyseal and metadiaphyseal area of the right proximal tibia with sunburst periosteal reaction on the lateral surface of the tibia.

B, C. Coronal T1-weighted spin-echo and axial T2-weighted fast spin-echo MR images demonstrate an extensive lesion occupying the nearly whole tibia with soft tissue component extending from the medullary space.

D. Gadolinium-enhanced axial T1-weighted spin-echo MR image obtained with fat saturation shows the homogenous enhancement of the entire lesion without a central necrotic portion.

E. Bone scan reveals the multiple areas of markedly increased activity.

가 : 가

가 가 (4) , 가

가 , , , (5) , , , 가

가

Bloom (3) 70%가 가

70 가 (8) Bloom (3) 4% (3/70)

3 가 4 가 Bloom (3) 70 가 6

1 가 Bloom

62

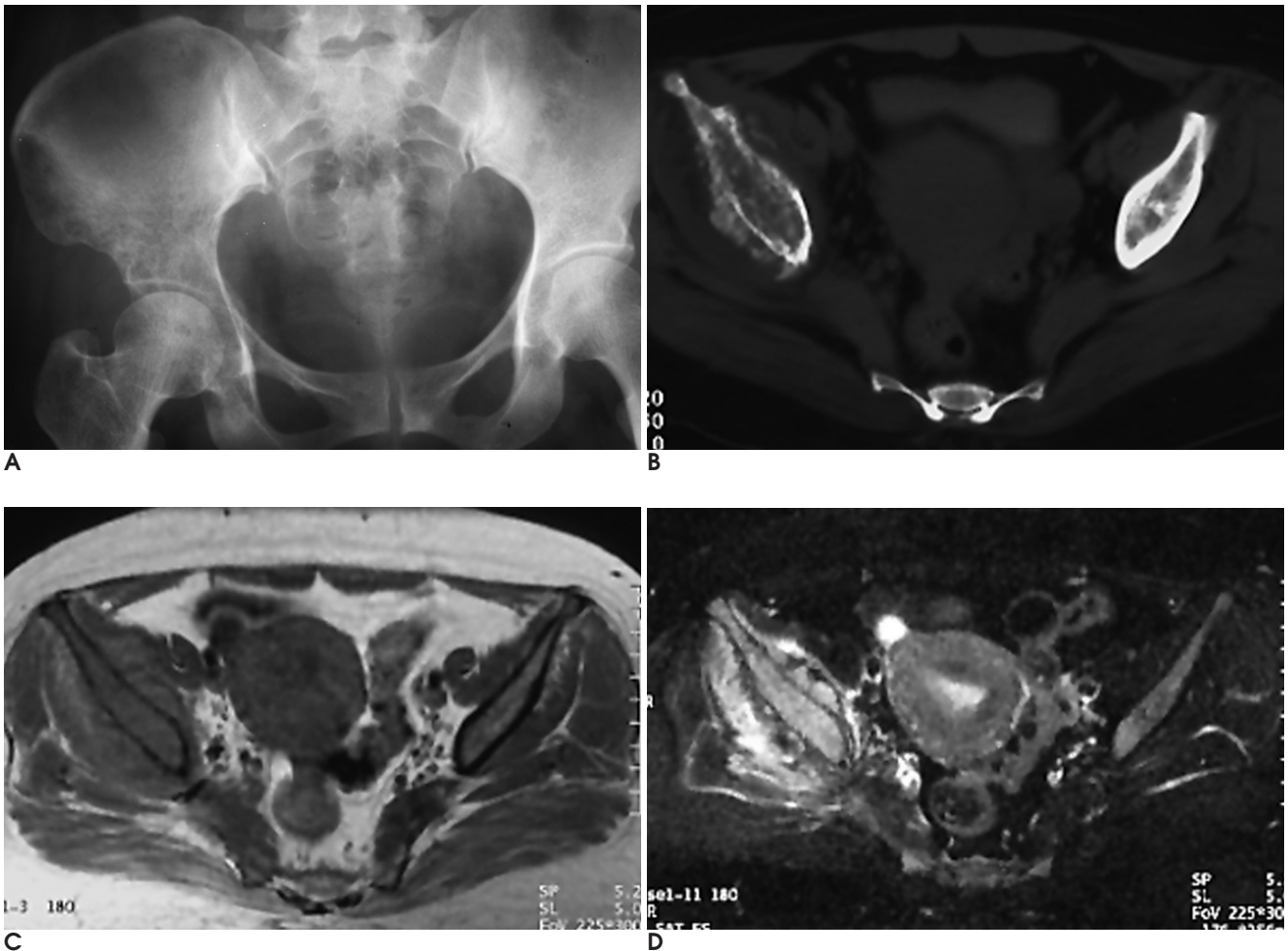


Fig. 2. A 50-year-old woman with lung adenocarcinoma.
A. Plain radiograph shows an ill-defined osteolytic lesion in the right iliac bone and acetabulum.
B. CT scan shows an ill-defined osteolytic lesion in the right iliac bone with sunburst periosteal reaction.
C. Axial T1-weighted spin-echo MR image reveals shows intermediate signal intensity lesion in the bone marrow of the right iliac bone with extraosseous soft tissue mass formation.
D. Axial fat-suppressed T2-weighted fast spin-echo MR image demonstrates high signal intensity of the bone marrow and extraosseous soft tissue mass.

70 (carcinoid) 1
1

가 (9).

가 .

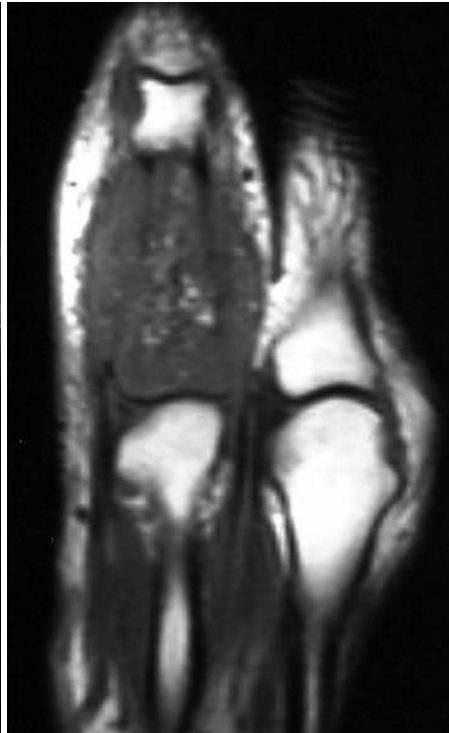
가 , , (11).

(7, 10). Bloom (3)

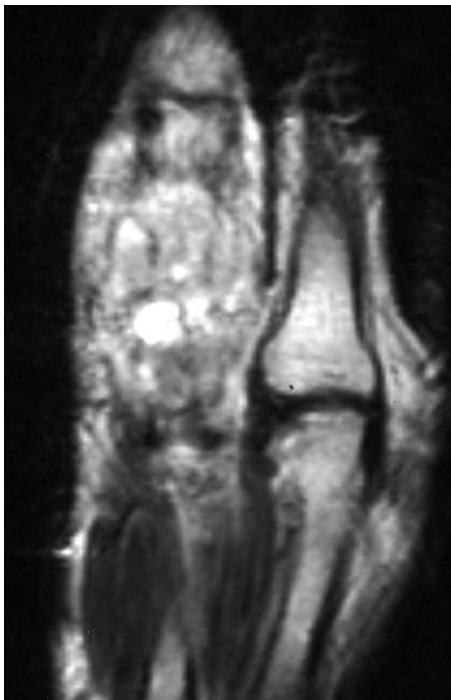
0.1%,



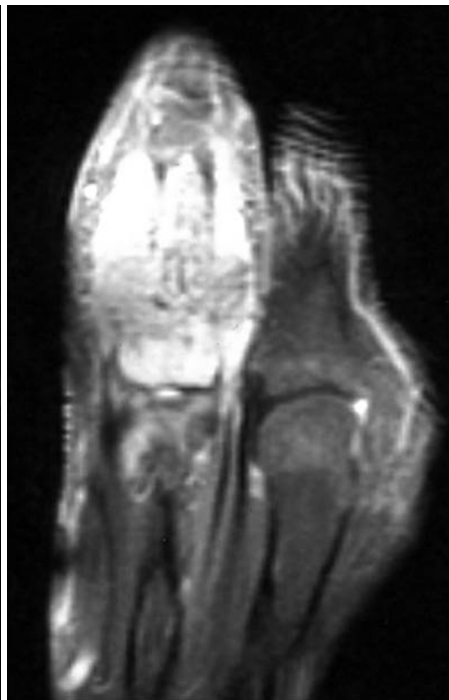
A



B



C



D

Fig. 3. A 53-year-old woman with stomach adenocarcinoma.

A. Plain radiograph shows the osteolytic bone destruction in the proximal phalanx of the right index with sunburst periosteal reaction.

B, C. Coronal T1-weighted spin-echo and coronal T2-weighted fast spin-echo MR images demonstrate an extensive lesion occupying almost entire proximal phalanx with soft tissue component extending from the medullary space. The masses were iso-intense on T1-weighted images as compared with muscle and heterogeneously hyperintense on T2-weighted images as compared with fat.

D. Gadolinium-enhanced coronal T1-weighted spin-echo MR image obtained with fat saturation shows the homogenous enhancement of the entire lesion without a central necrotic portion.

0.4% (12). Bloom (3)

20% (9, 15)

(14/70)

1 1 8

가

가

Milch (13)

Bloom (3)

가 6 , 가 3

가 가 (2).

(1 - 3).

(14). (5) 152

6
1

(tubular bone)

CT가

6 MRI 가 T1
MRI
, T2

1. Lehrer HZ, Maxfield WS, Nice CM. The periosteal "sunburst" pattern in metastatic bone tumors. *AJR Am J Roentgenol* 1970;108:154-161
2. Ragsdale BD, Madewell JE, Sweet DE. Radiologic and pathologic analysis of solitary bone lesions. Part II: periosteal reactions. *Radiol Clin North Am* 1981;19:749-783
3. Bloom RA, Libson E, Husband JE, Stoker DJ. The periosteal sunburst reaction to bone metastases. A literature review and report of 20 additional cases. *Skeletal Radiol* 1987;16:629-634
4. 1975;11:252-261
5. 152 1987;23:476-484
6. Nagendran T, Patel MN, Gaillard WE, Imm F, Walker M. Metastatic bronchogenic carcinoma to the bones of the hand. *Cancer* 1980;45:824-828
7. Yuh WT, Quets JP, Lee HJ, Simonson TM, Michalson LS, Nguyen PT, et al. Anatomic distribution of metastases in the vertebral body and modes of hematogenous spread. *Spine* 1996;21:2243-2250
8. Pagani JJ, Libshitz HI. Imaging bone metastases. *Radiol Clin North Am* 1982;20:545-560
9. Resnick D, Greenway GD. *Tumors and tumor-like lesions of bone: imaging and pathology of specific lesions*. In Resnick D. *Bone and Joint Imaging*. 2nd ed. Philadelphia: Saunders, 1996;991-1063
10. Sim FH, Pritchard DJ. Metastatic disease in the upper extremity. *Clin Orthop* 1982;169:83-94
11. Hove B, Gyldensted C. Spiculated vertebral metastases from prostatic carcinoma. Report of first two cases. *Neuroradiology* 1990;32:337-339
12. Healey JH, Turnbull AD, Miedema B, Lane JM. Acrometastases. A study of twenty-nine patients with osseous involvement of the hands and feet. *J Bone Joint Surg Am* 1986;68:743-746
13. Milch RA, Changus GW. Response of bone to tumor invasion. *Cancer* 1956;9:340-351
14. Edeiken J, Hodes PJ, Caplan LH. New bone production and periosteal reaction. *AJR Am J Roentgenol* 1966; 97:708-718
15. Boyko OB, Cory DA, Cohen MD, Provisor A, Mirkin D, DeRosa GP. MR imaging of osteogenic and Ewing's sarcoma. *AJR Am J Roentgenol* 1987;148:317-322

Metastatic Bone Tumors with Sunburst Periosteal Reaction¹

Gyung Kyu Lee, M.D., Hye Won Chung, M.D.², Heung Sik Kang, M.D.³,
Jin-Gyoon Park, M.D.⁴, Kil-Ho Cho, M.D.⁵, Young Hwan Lee, M.D.⁶,
Sung Moon Lee, M.D.⁷, Jongmin Lee, M.D.⁸, Jeong Mi Park, M.D.⁹, Ik Won Kang, M.D.,
Eil Seong Lee, M.D., Dae Hyun Hwang, M.D., Seon Jeong Min, M.D., Kyung Jin Suh, M.D.¹⁰

¹Department of Radiology, Hallym University College of Medicine, Hangang Sacred Heart Hospital

²Department of Radiology, Samsung Medical Center, Sungkyunkwan University College of Medicine

³Department of Radiology, Seoul National University Bundang Hospital

⁴Department of Radiology, Chonnam National University College of Medicine

⁵Department of Radiology, Yeungnam University College of Medicine

⁶Department of Radiology, Daegu Catholic University College of Medicine

⁷Department of Radiology, Keimyung University College of Medicine

⁸Department of Radiology, Kyungpook National University College of Medicine

⁹Department of Radiology, Catholic University College of Medicine

¹⁰Department of Radiology, Dankook University Hospital

Purpose: The purpose of this study was to describe the clinical and imaging features of metastatic bone tumors with sunburst periosteal reaction and to define the characteristic findings which would be helpful for differentiating metastatic bone tumors from primary malignant bone tumors.

Materials and Methods: The authors retrospectively reviewed the cases of nine patients with pathologically confirmed metastatic bone tumors with sunburst periosteal reaction, for which imaging studies (plain radiographs [$n=9$], radioisotope [RI] scans [$n=4$], magnetic resonance [MR] images [$n=6$], and computed tomographic [CT] scans [$n=4$]) were performed. The imaging studies of each lesion were analyzed by two musculoskeletal radiologists focusing on the metastatic site, patterns of bone response, signal intensity characteristics and pattern of contrast enhancement on MR. The clinical records of the patients were reviewed with regard to the age and sex of the subjects, the clinical presentation, and the origin of the primary tumors.

Results: The cases consisted of six men and three women, whose mean age was 62 years (age range, 50 - 88 years). The primary tumors were adenocarcinoma of the stomach [$n=4$], adenocarcinoma of the lung [$n=2$], adenocarcinoma of the prostate [$n=1$], hepatocellular carcinoma of the liver [$n=1$], and adenocarcinoma of unknown origin [$n=1$]. The sites of metastatic involvement exhibiting sunburst periosteal reaction were the scapula [$n=2$], proximal humerus [$n=2$], rib [$n=1$], iliac bone [$n=1$], tibia [$n=1$], spine [$n=1$], and proximal phalanx [$n=1$]. In all patients, the imaging findings showed osteolytic [$n=3$] or osteoblastic [$n=6$] lesions with sunburst periosteal reaction. In six cases, the lesions were iso-intense on the T1-weighted images and heterogeneously hyperintense on the T2-weighted images. The gadolinium-enhanced T1-weighted images showed a nearly homogenous enhancement of the lesions without any central necrotic portion.

Conclusion: Although metastatic bone tumor exhibiting sunburst periosteal reaction is rare, it should be included along with primary malignant bone tumors in the differential diagnosis of bone lesions with sunburst periosteal reaction, especially in older patients with or without a known primary malignancy.

Index words : Bone neoplasms, diagnosis
Bone neoplasms, secondary